

Spirostanol glycosides with hemostatic and antimicrobial activities from *Trillium kamtschaticum*

Yu Chen^{a, b, d}, Wei Ni^{a, d}, Huan Yan^{a, d}, Xu-Jie Qin^{a, d}, Afsar Khan^{a, c}, Hui Liu^{a, b, d}, Tong Shu^{a, b, d}, Ling-Yu Jin^{a, d}, Hai-Yang Liu^{a, d, *}

^a State Key Laboratory of Phytochemistry and Plant Resources in West China, Kunming Institute of Botany, Chinese Academy of Sciences, Kunming 650201, China

^b University of Chinese Academy of Sciences, Beijing 100039, China

^c Department of Chemistry, COMSATS Institute of Information Technology, Abbottabad 22060, Pakistan

^d Yunnan Key Laboratory of Natural Medicinal Chemistry, Kunming, 650201, China

ARTICLE INFO

Article history:

Received 21 March 2016

Received in revised form

2 September 2016

Accepted 12 September 2016

Available online 22 September 2016

Keywords:

Trillium kamtschaticum

Trilliaceae

Spirostanol glycosides

Hemostatic activity

Antimicrobial activity

ABSTRACT

Ten spirostanol glycosides, trillikamtosides A–J, together with eleven known analogues, were isolated from the hemostatic fraction of the 75% aqueous EtOH extract of the whole herbs of *Trillium kamtschaticum*. Their structures were established by extensive spectroscopic data analysis and chemical methods. The aglycones of three of these compounds had unique $3\beta,17\alpha$ -dihydroxy-spirostanes featuring a double bond between C-4 and C-5, while two others represent a rare class of spirostanol glycosides which possess a 5(6 → 7) abeo-steroidal aglycone. All the compounds were evaluated for their hemostatic and antimicrobial activities. Three of the spirostanol glycosides exhibited induced-platelet aggregation at a concentration of 300 $\mu\text{g}/\text{mL}$ with maximal induced-platelet aggregation rates of 72%, 71%, and 62% in rabbits, respectively, and their EC_{50} values were 492.7, 203.3, and 109.8 μM . Five of the spirostanol glycosides showed an anti-*Candida albicans* effect with MIC values of 21.1, 10.6, 8.8, 21.6, and 11.0 μM , respectively.

© 2016 Elsevier Ltd. All rights reserved.

1. Introduction

The genus *Trillium* (Trilliaceae) consists of approximately 49 species throughout the world, including 9 species in Asia and 40 found in North America (Ohara and Kawano, 2005). However, only three species (*T. kamtschaticum*, *T. tschonoskii*, and *T. govanianum*) are distributed in China. Some *Trillium* species have been used as folk remedies. The rhizome of *T. erectum* (Beth root), for example, is commonly used as women's herb to aid childbirth and to treat irregular menstrual periods in various native North American Indian tribes (Hayes et al., 2009). The rhizomes of *T. kamtschaticum* and *T. tschonoskii*, called “Toudingyikezhu” in Chinese, have been used as a traditional Chinese medicine usually to treat hypertension, waist and leg pain, as well as traumatic hemorrhage (Jiangsu New Medical College, 1975; Wang et al., 1978). Moreover, some

Chinese minorities, namely the Tujia and Miao people, traditionally use *T. tschonoskii* to promote blood flow for regulating menstruation and to treat traumatic hemorrhage (Zhang et al., 2011). In recent pharmacological studies, the crude extract of this species showed anti-inflammatory, analgesic, and procoagulant effects (Yu et al., 2008). Although some phytochemical investigations on *Trillium* plants have been reported (Ono et al., 2003, 2007; Yokosuka and Mimaki, 2008), their hemostatic components are still not clear.

The preliminary pharmacological study herein established that the crude extract of the whole plants of *T. kamtschaticum* exhibited significant induced-platelet aggregation activity at a concentration of 1.5 mg/mL. In an ongoing search to identify bioactive constituents, a macroporous resin column was used to obtain 30%, 70%, and 95% aqueous EtOH eluted fractions. The 70% EtOH fraction showed 76% maximal platelet aggregation rate at a concentration of 1.5 mg/mL, while the other two fractions did not induce platelet aggregation activity obviously. With the aim of searching for bioactive constituents, the 70% EtOH eluent was investigated further, resulting in the isolation of ten new spirostane-type saponins, trillikamtosides A–J (1–10) (Fig. 1), and 11 known analogues:

* Corresponding author. State Key Laboratory of Phytochemistry and Plant Resources in West China, Kunming Institute of Botany, Chinese Academy of Sciences, Kunming 650201, China.

E-mail address: haiyangliu@mail.kib.ac.cn (H.-Y. Liu).

pennogenin 3-O- β -D-glucopyranoside (**11**) (Ono et al., 2007), pennogenin 3-O- α -L-rhamnopyranosyl-(1 \rightarrow 2)- β -D-glucopyranoside (**12**) (Nohara et al., 1975; Ono et al., 2007), floribundasaponin B (**13**) (Mahato et al., 1981), pennogenin 3-O- β -chacotrioside (**14**) (Nohara et al., 1975), pennogenin 3-O- α -L-rhamnopyranosyl-(1 \rightarrow 4)- α -L-rhamnopyranosyl-(1 \rightarrow 4)- β -D-glucopyranoside (**15**) (Mimaki et al., 2000), pennogenin 3-O- α -L-rhamnopyranosyl-(1 \rightarrow 4)- α -L-rhamnopyranosyl-(1 \rightarrow 4)-[α -L-rhamnopyranosyl-(1 \rightarrow 2)]- β -D-glucopyranoside (**16**) (Nohara et al., 1975), polyphyllin V (**17**) (Chen et al., 1981), ophiopogonin B (**18**) (Asano et al., 1993), (25S)-27-hydroxypennogenin 3-O- β -D-glucopyranoside (**19**) (Yokosuka and Mimaki, 2008), (25S)-27-hydroxypennogenin-3-O- α -L-rhamnopyranosyl-(1 \rightarrow 2)- β -D-glucopyranoside (**20**) (Ono et al., 2007), and trikamsteroside A (**21**) (Ono et al., 2007), respectively. All of the purified compounds were evaluated for their hemostatic effects using the induced-platelet aggregation assay. Furthermore, the antimicrobial activities of all the glycosides were tested. Herein, the isolation, structural elucidation, and bioactivities of these isolates are described.

2. Results and discussion

Trillikamtoside A (**1**) was obtained as a white amorphous powder. Its molecular formula was deduced as C₃₉H₆₂O₁₄ on the basis of its HR-EI-MS ion peak at m/z 754.4162 [M]⁺ (calcd. 754.4140) and its ¹³C NMR data (Table 3), requiring nine degrees of unsaturation. The presence of hydroxy and double bond functionalities was deduced from the IR absorption bands at 3423 and 1636 cm⁻¹. The ¹H NMR spectrum of **1** exhibited signals for four characteristic steroidal methyls at δ_H 0.68 (d, J = 4.6 Hz), 1.01 (s), 1.61 (s), and 1.24 (d, J = 6.8 Hz) and one olefinic proton at δ_H 5.93 (br s), as well as two anomeric protons at δ_H 5.02 (d, J = 7.8 Hz) and 6.32 (br s). The ¹³C NMR spectrum (Table 3) showed a total of 39 carbon signals, which were ascribed to five methyls, 10 methylenes (including two oxygenated ones), 18 methines (including 13 oxygenated ones), three quaternary carbons (including an oxygenated one at δ_C 90.4), a trisubstituted double bond, and one ketal carbon at δ_C 110.3. The double bond and the two monosaccharide units in compound **1** accounted for three degrees of unsaturation, and the remaining six ones of unsaturation required that the aglycone of **1** should be a hexacyclic-ring system. The spectroscopic data of C-16 (δ_C 90.5) and C-17 (δ_C 90.4) suggested it was a 17-hydroxylated spirostane-type derivative (Nohara et al., 1975).

Careful analysis of the 1D- and 2D-NMR data for the aglycone of **1** disclosed that it contained the same C–F rings as pennogenin in compounds **11**–**16** (Ono et al., 2007). However, the main differences were observed in A- and B-rings, as well as the presence of an additional oxygenated methine (δ_H 4.48; δ_C 74.1). Key ¹H–¹H COSY correlations (Fig. 2) of δ_H 5.93 (H-4)/ δ_H 4.43 (H-3) and δ_H 4.48 (H-6)/ δ_H 1.25 and 2.21 (H₂-7) suggested location of a double bond at C-4/C-5 and the oxygenated methine at C-6, respectively. This was also supported by HMBC correlations (Fig. 2) from H-4 to C-2, C-6, and C-10, from H-6 to C-4, C-8, and C-10, from Me-19 to C-1, C-5, and C-9. The β -orientation of the OH-6 was deduced from ROESY correlations of δ_H 5.93 (H-4)/4.48 (H-6), 0.88 (H-9)/1.25 (H-7), 4.48 (H-6)/1.25 (H-7). The other parts were determined to be the same as those of pennogenin by 2D NMR experiments. Based on the above evidence, the aglycone of **1** was elucidated as (25R)-spirost-4-ene-3 β ,6 β ,17 α -triol.

Acid hydrolysis of **1** gave D-glucose and L-rhamnose, as determined by HPLC analysis of their L-cysteine methyl esters followed by conversion into *o*-tolyl isothiocyanate derivatives. The large coupling constant (³ $J_{1,2}$ = 7.8 Hz) of the anomeric proton of the D-glucopyranosyl moiety suggested that it was β -orientated, while

the α -orientation for the L-rhamnopyranosyl unit was defined by its chemical shift values of C-3'' (δ_C 73.1) and C-5'' (δ_C 69.6) with those of the corresponding carbons of methyl α - and β -rhamnopyranoside (Kasai et al., 1979). HMBC correlations of δ_H 5.02 (H-1') with δ_C 75.2 (C-3) and of δ_H 6.32 (H-1'') with δ_C 78.6 (C-2') enabled identification of the location of the saccharide chain to C-3, whereas the rhamnopyranosyl was attached to C-2' of the glucopyranosyl moiety. Therefore, structure **1** was elucidated as (25R)-spirost-4-ene-3 β ,6 β ,17 α -triol-3-O- α -L-rhamnopyranosyl-(1 \rightarrow 2)- β -D-glucopyranoside.

Trillikamtoside B (**2**) was isolated as a white amorphous powder with molecular formula C₄₅H₇₂O₁₈, as determined by the HR-ESI-MS data exhibiting an [M + Na]⁺ peak at m/z 923.4625 and its ¹³C NMR data (Table 3). By comparing its ¹H and ¹³C NMR data (Tables 1 and 3) with those of **1**, compound **2** was deduced to have the same aglycone as **1**. Three monosaccharide moieties were present in structure **2** according to the three anomeric protons at δ_H 4.91 (d, J = 7.6 Hz, H-1'), 5.87 (br s, H-1'''), and 6.33 (br s, H-1'') and the corresponding anomeric carbons at δ_C 100.4 (C-1'), 102.8 (C-1'''), and 102.1 (C-1''). The sugars units were determined to be a glucopyranosyl moiety and two rhamnopyranosyls by its ¹H- and ¹³C-NMR, HSQC, HMBC, and ROESY experiments, which was further confirmed by acid hydrolysis and HPLC analysis. The sequence of the trisaccharide chain at C-3 of the aglycone was established from the following HMBC correlations: H-1' (δ_H 4.91) of Glc with C-3 (δ_C 74.6) of the aglycone, H-1'' (δ_H 6.33) of the inner Rha with C-2' (δ_C 77.8) of Glc, and H-1''' (δ_H 5.87) of the terminal Rha with C-4' (δ_C 78.2) of Glc. Thus, structure **2** was elucidated as (25R)-spirost-4-ene-3 β ,6 β ,17 α -triol-3-O- α -L-rhamnopyranosyl-(1 \rightarrow 4)-[α -L-rhamnopyranosyl-(1 \rightarrow 2)]- β -D-glucopyranoside.

Trillikamtoside C (**3**) had a molecular formula of C₃₉H₆₀O₁₄, based on the HR-ESI-MS data (m/z 775.3875 [M + Na]⁺). Overall, the NMR features of **3** showed a high similarity to those of **1**, except for the replacement of the oxymethine (δ_C 74.1) at C-6 by an unsaturated ketone group (δ_C 203.0) in **3**. Its UV absorption at 240 nm supported that **3** possessed an α,β -unsaturated ketone substructure. This observation was verified by HMBC correlations from H-4 (δ_H 6.56), H₂-7 (δ_H 2.54, 1.92), and H-8 (δ_H 1.90) to C-6 (δ_C 203.0). Consequently, structure **3** was identified as (25R)-3 β ,17 α -dihydroxyspirost-4-ene-6-one-3-O- α -L-rhamnopyranosyl-(1 \rightarrow 2)- β -D-glucopyranoside.

Trillikamtoside D (**4**) showed a molecular of C₃₉H₆₀O₁₄, as evidenced from the HR-ESI-MS data (m/z 775.3876 [M + Na]⁺). Its UV spectrum showed absorption maxima at 255 nm, indicating the presence of a conjugated enal system (Lu et al., 2010), while its IR spectrum with absorptions at 3425 and 1664 cm⁻¹ suggested the existence of hydroxy and olefin groups, respectively. The ¹H NMR and ¹³C NMR spectroscopic data (Tables 1 and 3) of **4** exhibited signals of an aldehyde (δ_H 10.3, δ_C 189.8), a tetrasubstituted double bond (δ_C 140.4 and 170.3) and other typical resonances of steroidal saponins. Comparison of all signals of **4** with ypsilandroside H (Lu et al., 2010) showed they had the same skeleton of B-nor(7)-6-carboxaldehyde-spirost-5(7)-en. The HMBC correlations (Fig. 2) of δ_H 0.87 (Me-19) with δ_C 170.3 (C-5), δ_H 4.07, 2.53 (H₂-4) with δ_C 140.4 (C-7), and δ_H 10.3 (H-6) with δ_C 170.3 (C-5) and 46.8 (C-8) also indicated the basic structure of **4**. Its sugar residues were determined to be the same as those of **1** and **3** based on NMR data, which were confirmed by its acid hydrolysis. The sequence of the disaccharide attached to C-3 was further proved by the observed HMBC correlations of H-1' (δ_H 5.12) of the glucopyranosyl moiety with C-3 (δ_C 78.2) of the aglycone, and H-1'' (δ_H 6.47) of the rhamnopyranosyl unit with C-2' (δ_C 77.7) of the Glc. Thus, compound **4** was characterized as (25R)-B-nor(7)-6-carboxaldehyde-spirost-5(7)-en-3 β -O- α -L-rhamnopyranosyl-(1 \rightarrow 2)- β -D-glucopyranoside.

Trillikamtoside E (**5**) had the molecular formula C₄₅H₇₀O₁₈ based

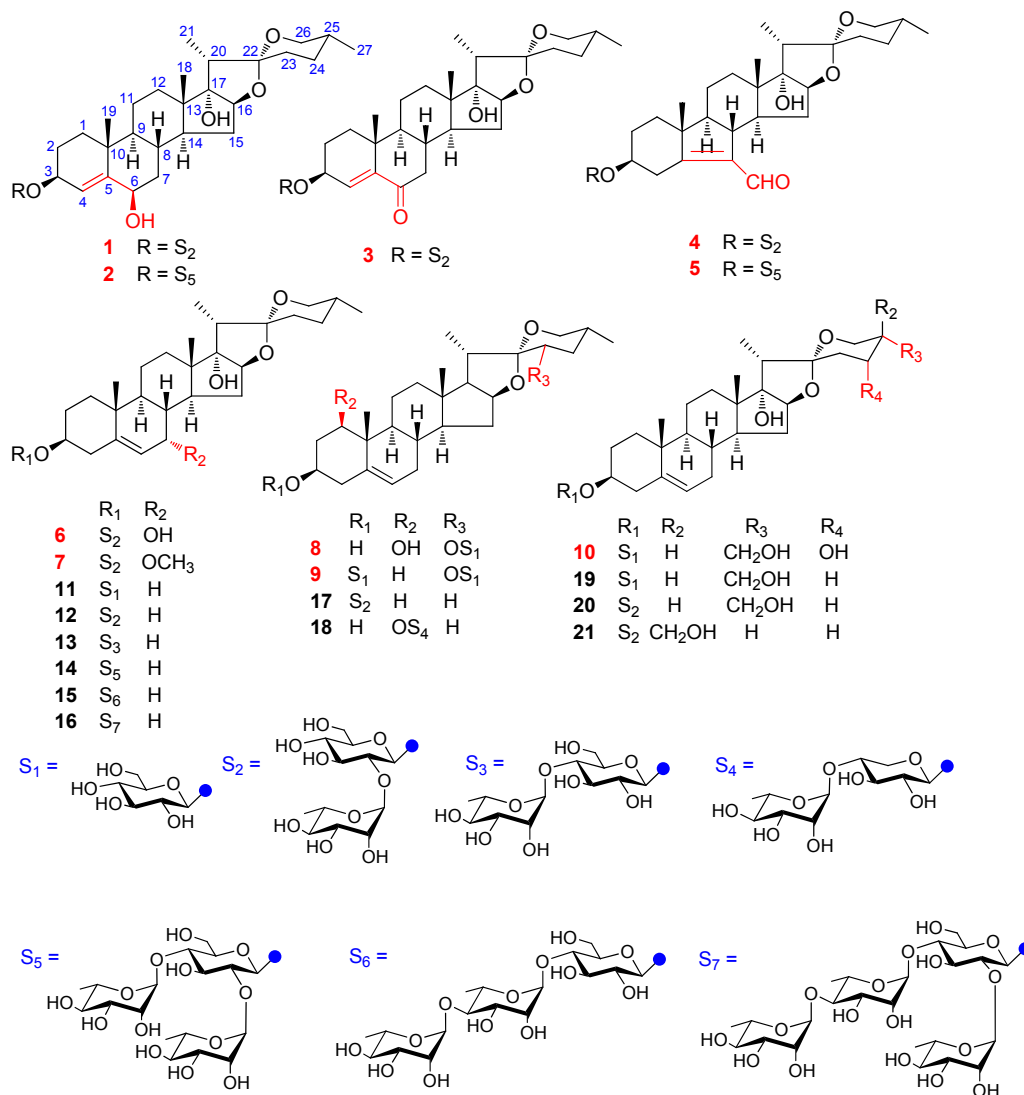
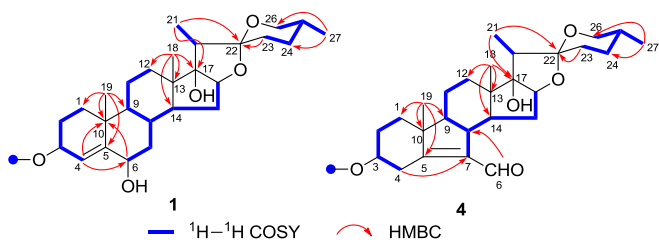


Fig. 1. Structures of compounds 1–21.

Fig. 2. Key HMBC and ¹H–¹H COSY correlations of the aglycone moieties for **1** and **4**.

on HR-ESI-MS data (m/z 921.4453 [$M + Na$]⁺). Moreover, the ¹³C-NMR and DEPT spectroscopic data (Table 3) showed compound **5** sharing the same aglycone as **4**. Its ¹H NMR spectrum (Table 1) displayed signals for three anomeric protons (δ_H 5.02, 5.88, and 6.48) and the ¹³C NMR chemical shifts (Table 3) of sugar units of **5** were similar as those of **2**. Thus, compound **5** was determined as (25*R*)-B-nor(7)-6-carboxaldehyde-spirost-5(7)-en-3 β - α -L-rhamnopyranosyl-(1 → 4)-[α -L-rhamnopyranosyl-(1 → 2)]- β -D-glucopyranoside.

Trillikamtoside F (**6**) exhibited a molecular formula of C₃₉H₆₂O₁₄

as determined by the positive HR-ESI-MS ion peak at m/z 777.4042 [$M + Na$]⁺ (calcd. 777.4037) and the ¹³C NMR data (Table 3). Comparison of the NMR spectroscopic data (Tables 2 and 3) of **6** with those of pennogenin 3-*O*- α -L-rhamnopyranosyl-(1 → 2)- β -D-glucopyranoside (**12**) (its ¹³C NMR data see Supplementary material S11) indicated that they were very similar, except for the presence of an additional oxymethine (δ_H 4.05, br s; δ_C 64.5) and the absence of a methylene in **6**. The oxymethine was placed at C-7 on the basis of the ¹H–¹H COSY correlation of δ_H 5.75 (H-6) with δ_H 4.05 (H-7). The relative configuration of OH-7 was determined to be α -oriented by the chemical shift of C-7 (δ_C 64.5), while the signals for C-7 would be at δ_C 73.2 for the β -OH isomer (Zhang et al., 2012). The sugar part of **6** was determined to be the same as those of **1**, **3**, and **4** by detailed analysis of their NMR spectroscopic data. Based on the above evidence, structure **6** was defined as (25*R*)-spirost-5-ene-3 β ,7 α ,17 α -triol 3-*O*- α -L-rhamnopyranosyl-(1 → 2)- β -D-glucopyranoside.

Trillikamtoside G (**7**) displayed an ion peak at m/z 791.4188 [$M + Na$]⁺ (calcd. for, C₄₀H₆₄O₁₄Na, 791.4194) in the HR-ESI-MS, being 14 mass units more than **6**. Its ¹H and ¹³C NMR spectroscopic data showed its structure resembling that of **6** with the main difference of an extra methoxy group signals (δ_H 3.23; δ_C 56.2). The

Table 1
¹H NMR spectroscopic data of **1–5** in C₅D₅N (δ_H, mult, J in Hz).^a

Position	1 ^b	2 ^b	3 ^c	4 ^b	5 ^b
1a	1.66, o	1.62, o	1.53, m	1.70, m	1.68, m
1b	1.17, t (13.4)	1.15, t (13.5)	1.15, t (13.4)	1.10, dd (12.3, 3.4)	1.10, dd (13.2, 3.4)
2a	2.03, br s	1.99, br d (3.6)	2.09, o	2.25, brd (12.4)	2.15, dd (11.8, 3.4)
2b	1.94, q (11.8)	1.88, q (11.8)	1.82, q (11.8)	1.96, q (11.8)	1.89, q (11.8)
3	4.43, m	4.43, m	4.50, m	4.33, q (8.8)	4.02, q (8.8)
4a	5.93, br s	5.87, br s	6.56, br s	4.07, m	4.05, m
4b				2.53, td (12.2, 3.5)	2.49, t (13.0)
6	4.48, o	4.43, o		10.3, s	10.3, s
7a	2.21, q (13.2)	2.18, q (13.8)	2.54, br d (11.8)		
7b	1.25, m	1.20, m	1.92, q (12.0)		
8	2.43, q (9.0)	2.40, q (10.8)	1.90, m	2.76, td (11.0, 3.8)	2.75, td (11.0, 3.8)
9	0.88, t (9.6)	0.84, t (9.6)	1.09, td (11.6, 3.6)	1.16, td (11.4, 4.0)	1.15, td (11.4, 4.0)
11a	1.60, o	1.57, o	1.53, m	1.45, o	1.44, o
11b	1.54, o	1.50, o	1.33, ddd (3.6, 13.2, 14.6)	1.45, o	1.44, o
12a	2.21, q (13.2)	2.18, q (13.8)	2.18, o	2.18, td (12.6, 5.2)	2.16, m
12b	1.55, o	1.55, o	1.54, o	1.53, brd (12.8)	1.51, brd (12.8)
14	2.17, m	2.13, m	2.14, m	2.44, td (12.8, 6.8)	2.43, td (13.0, 6.0)
15a	2.31, m	2.27, m	2.10, m	2.89, m	2.86, m
15b	1.57, o	1.55, o	1.49, q (7.0)	2.10, td (13.0, 6.0)	2.10, td (13.0, 6.0)
16	4.48, o	4.44, t (7.2)	4.42, t (7.2)	4.50, t (8.3)	4.48, t (7.2)
17					
18	1.01, s	0.98, s	0.93, s	1.03, s	1.05, s
19	1.61, s	1.58, s	0.93, s	0.87, s	0.86, s
20	2.28, q (7.2)	2.25, q (7.2)	2.25, q (7.2)	2.30, q (7.2)	2.28, q (7.0)
21	1.24, d (6.8)	1.20, d (6.8)	1.21, d (6.8)	1.25, d (7.2)	1.24, d (7.2)
23a	1.71, o	1.67, o	1.70, o	1.73, o	1.73, o
23b	1.65, o	1.59, o	1.65, o	1.73, o	1.73, o
24a	1.55, o	1.54, o	1.55, o	1.58, o	1.58, o
24b	1.55, o	1.54, o	1.55, o	1.58, o	1.58, o
25	1.55, o	1.55, o	1.55, o	1.62, o	1.58, o
26a	3.50, o	3.48, o	3.48, o	3.52, o	3.50, o
26b	3.50, o	3.48, o	3.48, o	3.52, o	3.50, o
27	0.68, d (4.6)	0.65, d (5.4)	0.65, d (5.4)	0.72, d (6.0)	0.70, d (6.0)
3-O-Glc					
1'	5.02, d (7.8)	4.91, d (7.6)	4.95, d (7.8)	5.12, d (7.3)	5.02, d (7.2)
2'	4.26, t (8.3)	4.23, o	4.18, o	4.34, o	4.37, o
3'	4.33, q (8.0)	4.18, q (8.0)	4.24, q (9.0)	4.32, dd (12.8, 8.0)	4.22, o
4'	4.18, t (9.0)	4.38, o	4.09, t (9.0)	4.20, t (9.1)	4.42, o
5'	3.97, br s	3.71, br d (9.6)	3.91, o	3.96, br d (9.4)	3.67, br d (9.4)
6'a	4.59, o	4.26, m	4.54, m	4.58, br d (11.8)	4.25, m
6'b	4.41, m	4.10, br d (11.8)	4.32, m	4.39, m	4.10, m
2'-O-Rha					
1''	6.32, br s	6.33, br s	6.25, br s	6.47, br s	6.48, br s
2''	4.82, br s	4.84, br s	4.78, br s	4.81, br s	4.84, br s
3''	4.56, o	4.54, o	4.62, dd (9.6, 3.0)	4.66, dd (9.0, 3.0)	4.63, dd (9.2, 3.0)
4''	4.33, m	4.34, o	4.25, o	4.37, o	4.38, o
5''	4.93, t (6.3)	4.86, o	4.71, o	5.03, o	4.97, o
6''	1.72, d (4.8)	1.67, d (6.0)	1.68, d (6.0)	1.77, d (6.0)	1.75, d (6.5)
4'-O-Rha					
1'''		5.87, br s			5.88, br s
2'''		4.70, br s			4.70, br s
3'''		4.54, o			4.57, dd (9.2, 3.0)
4'''		4.34, o			4.38, o
5'''		4.96, t (7.6)			4.98, o
6'''		1.62, d (6.6)			1.65, d (6.6)

^a s, singlet; d, doublet; t, triplet; q, quartet; br, broad; m, multiplet; o, overlapped.

^b Recorded at 600 MHz.

^c Recorded at 400 MHz.

methoxy functionality was assigned to be at C-7 by the HMBC correlations of δ_H 3.23 with δ_C 73.6 (C-7). The ROESY correlation between 7-OMe (δ_H 3.23)/H-14 (δ_H 2.83) indicated that the methoxy moiety was α-oriented. Consequently, structure **7** was elucidated to be (25*R*)-spirost-5-ene-3β,17α-diol-7α-methoxy-3-*O*-α-*L*-rhamnopyranosyl-(1 → 2)-β-*D*-glucopyranoside.

Trillikamtoside H (**8**) was assigned the molecular formula C₃₃H₅₂O₁₀ based on the HR-ESI-MS analysis (*m/z* 631.3461 [M + Na]⁺). Comparison of the NMR data of **8** with those of aculeoside B (Mimaki et al., 1998) showed that it had the same overall structure, except for the absence of a sugar moiety at C-1. This was

supported by the upfield chemical shift of C-1 (δ_C 85.1 ppm → 78.1 ppm) and the long-range correlation of the anomeric proton signal at δ_H 5.00 (H-1') with the carbon resonance at δ_C 76.4 (C-23) in the HMBC spectrum. ROESY correlations suggested the same relative configuration as aculeoside B. Accordingly, structure **8** was confirmed as (23*S*,25*R*)-spirost-5-ene-1β,3β,23-triol-23-*O*-β-*D*-glucopyranoside.

Trillikamtoside I (**9**) showed a molecular of C₃₉H₆₂O₁₄ by the HR-ESI-MS (*m/z* 777.4045 [M + Na]⁺) and its ¹³C NMR data (Table 3). Its ¹H and ¹³C NMR spectroscopic data (Tables 2 and 3) verified that it was similar to compound **8** with a glucosylated C-23. The ¹H and

^{13}C NMR spectroscopic data of the aglycone of **9** (Tables 2 and 3) indicated that the basic skeleton of **9** was similar to diosgenin in compound **17** (its ^{13}C NMR data see Supplementary material S12), except for presence of an oxygenated methine (δ_{H} 4.06; δ_{C} 76.6) and the absence of a methylene in F-ring. The oxymethine was assigned to be C-23 on the grounds of the ^1H - ^1H COSY of H-23 (δ_{H} 4.06) with H₂-24 (δ_{H} 1.91 and 2.41), of H₂-24 with H-25 (δ_{H} 1.81) and the HMBC correlations from H-20 (δ_{H} 3.24) to C-23 (δ_{C} 76.6). The 23S configuration was deduced from ROESY correlations of H-23 (δ_{H} 4.06)/H-20 (δ_{H} 3.24) and H-23/H-25 (δ_{H} 1.81). Furthermore, two glucopyranosyl moieties were identified by extensive 1D and 2D NMR analysis, and hydrolysis. The HMBC correlation of δ_{H} 5.04 (H-1') of 3-Glc with δ_{C} 78.1 (C-3) of the aglycone, and δ_{H} 5.00 (H-1'') of 23-Glc with δ_{C} 76.6 (C-23) of the aglycone, indicated that C-3 and C-23 were glycosylated, and **9** was a bisdesmoside. Thus, structure **9** was defined as (23S,25R)-23-O- β -D-glucopyranosyl-spirost-5-ene-3 β ,23-diol-3-O- β -D-glucopyranoside.

Trillikamtoside J (**10**) displayed a molecular of $\text{C}_{33}\text{H}_{52}\text{O}_{11}$ as determined by HR-ESI-MS (m/z 647.3397 [$\text{M} + \text{Na}$] $^+$). Its ^{13}C NMR data (Table 3) suggested that its aglycone was a 17 α ,27-dihydroxy- Δ^5 -spirostane (Yokosuka and Mimaki, 2008) with an additional oxymethine (δ_{C} 66.3). The ^1H - ^1H COSY correlations of H-24 (δ_{H} 4.55)/H-25 (δ_{H} 2.25) and an HMBC correlation from H_a-27 (δ_{H} 4.38) to δ_{C} 66.3 (C-24) verified the presence of a 24-OH group. Its 24R and 25S configurations were determined by ROESY correlations of H-23ax (δ_{H} 2.11)/H-20 (δ_{H} 2.39), H-23ax/H-21 (δ_{H} 1.28), H-24 (δ_{H} 4.55)/H-23ax, and H-25 (δ_{H} 2.25)/H-23ax. Furthermore, detailed analysis of 1D and 2D NMR spectra showed that the sugar moiety of **10** was a glucopyranosyl moiety. Based on this evidence, structure **10** was established as (24R,25S)-spirost-5-ene-3 β ,17 α ,24,27-tetraol-3-O- β -D-glucopyranoside.

Considering the fact that steroidal glycosides show antimicrobial (Qin et al., 2012, 2013) and induced rabbit platelet aggregation (Sun et al., 2014) properties, all of the compounds were evaluated for hemostatic and antimicrobial effects against one fungal (*Candida albicans*) and three bacterial strains (*Staphylococcus aureus*, *Escherichia coli*, and *Pseudomonas aeruginosa*) (Table 4). Pennogenin-type saponins **12**, **14**, and **16** showed maximal induced-platelet aggregation rates (MPAR) of 72%, 71%, and 62% with EC₅₀ values of 492.7 \pm 33.3, 203.3 \pm 29.9, and 109.8 \pm 45.4 μM , respectively. This finding suggested that the hydroxy group at C-17 in pennogenin glycosides was essential towards the hemostatic effect, whereas the introduction of different functional groups in the A, B, or F-ring of pennogenin glycosides could make the hemostatic effect weak or disappear. In addition, the type of monosaccharide, the length of sugar moiety, and the linkage of sugar sequence attached to penogenin also had an effect on hemostatic activity. Moreover, **12**, **13**, **14**, **17**, and **18** exhibited significant antifungal effects against *C. albicans* with MIC values of 21.1, 10.6, 8.8, 21.6, and 11.0 μM , respectively, compared to positive control fluconazole (MIC 52.3 μM). None of the compounds showed antibacterial effects against the selected bacteria as compared to vancomycin and amikacin.

3. Conclusion

The present phytochemical investigation of the bioactive part of *T. kamtschaticum* led to isolation of 21 spirostane-type steroidal glycosides. Among them, 17 compounds were elucidated as pennogenin glycosides and their derivatives, and the remaining four were diosgenin glycosides and their derivatives. The aglycones of **1**–**3** have a unique 3 β ,17 α -dihydroxy-spirostane skeleton containing a double bond between C-4 and C-5, while **4** and **5** possess a rare 5(6 \rightarrow 7) abeo-steroidal aglycone containing a 6-5-6-5-5-6 fused ring spirostane with an α,β -unsaturated aldehyde group in B

ring. This is the first report of pennogenin glycosides being responsible for the hemostatic effect of title species, which also supports its traditional use as a hemostatic agent.

4. Experimental

4.1. General experimental procedures

Optical rotations were measured on a SEPA-3000 automatic digital polarimeter. EI-MS and HR-EI-MS were recorded on Waters AutoSpec Premier P776. ESI-MS spectra were obtained on a Bruker HTC/Esquire spectrometer. HR-ESI-MS spectra were acquired on an API QStar Pulsar instrument. IR spectra were measured on a Bio-Rad FTS-135 spectrometer with KBr pellets, whereas UV spectra were obtained using a Shimadzu UV-2401PC spectrophotometer. NMR spectra were run on Bruker DRX-500 and Avance III 600 instruments with TMS as internal standard. Column chromatography (CC) was performed over silica gel (200–300 mesh, 10–40 μm , Qingdao Marine Chemical Co., China), RP-18 (40–63 μm , Merck), and Sephadex LH-20 (GE Healthcare, Sweden). TLC was performed on HSGF₂₅₄ (0.2 mm, Qingdao Marine Chemical Co., China) or RP-18 F₂₅₄ (0.25 mm, Merck). Fractions were monitored by TLC and spots were visualized by heating silica gel plates after spraying with 10% H₂SO₄ in EtOH. Semi-preparative HPLC was run on an Agilent 1100 liquid chromatograph with a diode array detector (DAD) setting of 203 and 254 nm, and using a ZORBAX SB-C₁₈ (5 μm) column (250 \times 9.4 mm i.d.). Analytical HPLC analysis was carried out on an Agilent 1100 liquid chromatograph with diode array detector (DAD) setting at 203 nm and 254 nm, ZORBAX SB-C₁₈ (5 μm) column (250 \times 4.6 mm i.d.). Turbidometric measurements of platelet aggregation of the samples were performed in a Chrono-log Model 700 Aggregometer (Chrono-log Corporation, Havertown, PA, USA).

4.2. Plant material

Whole plants of *T. kamtschaticum* were collected in July 2012 from Panshi city, Jilin Province, China, and identified by Dr. Yun-Heng Ji of the Kunming Institute of Botany. A voucher specimen (No. HY0016) is deposited at the State Key Laboratory of Phytochemistry and Plant Resources in West China, Kunming Institute of Botany, CAS.

4.3. Extraction and isolation

Air-dried and powdered plant material (10.0 kg) was extracted with EtOH/H₂O (75:25, v/v, 3 \times 20 L), with solvent extraction carried out under conditions of reflux for a total of 6 h (3 \times 2 h). The combined extracts were concentrated under reduced pressure, then extracted with *n*-BuOH (20 L \times 3). The evaporated combined *n*-BuOH extracts (1.2 kg) were subjected to D101 macroporous resin CC eluted successively with an EtOH:H₂O gradient system (0:100; 30:70; 70:30; 95:5, v/v). The EtOH:H₂O (70:30, v/v) fraction (270.2 g) was passed through an MCI gel column and subsequently through a silica gel column (200–300 mesh) with gradients of CHCl₃:MeOH:H₂O (10:1:0; 8:2:0.2; 7:3:0.5; and 2:1:0.5, v/v) to give four fractions (Fr. 1–Fr. 4). Fr. 2 (97.8 g) was further subjected to MPLC (RP-18; MeOH:H₂O, 50:50 \rightarrow 90:10, v/v) to give six sub-fractions (Fr. 2.1–Fr. 2.6). Compounds **12** (10.0 mg) and **17** (23.5 mg) were obtained from Fr.2.2 (15.5 g) after repeated silica gel CC (CHCl₃:MeOH, 20:1 \rightarrow 10:1, v/v). Fr. 2.3 (19.8 g) and Fr. 2.4 (10.3 g) were subjected to Sephadex LH-20 CC (MeOH:CHCl₃, 1:1, v/v) followed by semi-preparative HPLC to yield **11** (2.0 mg), **13** (13.5 mg), **15** (7.6 mg), and **18** (20.9 mg). Fr. 3 (86.0 g) was applied to MPLC (RP-18; MeOH:H₂O, 60:40 \rightarrow 100:0, v/v) separately to give five subfractions (Fr. 3.1–Fr. 3.5). Likewise, Fr. 3.1 (33.3 g) was subjected

Table 2
¹H NMR spectroscopic data of **6–10** in C₅D₅N (δ_H, mult, *J* in Hz).^a

Position	6 ^b	7 ^b	8 ^c	9 ^c	10 ^b
1a	1.70, m	1.69, m	3.70, d (10.4)	1.65, m	1.69, m
1b	0.89, td (13.8, 3.0)	0.96, o		0.92, dd (13.6, 3.0)	0.92, o
2a	2.02, m	2.06, br d (13.8)	2.58, br d (11.4)	2.12, br d (11.6)	2.12, brd (11.2)
2b	1.87, q (11.8)	1.87, q (11.8)	2.22, q (11.8)	1.71, o	1.72, m
3	3.83, m	3.91, m	3.94, m	3.94, m	3.88, m
4a	2.83, br d (8.0)	2.89, dd (13.6, 4.6)	2.65, q (12.0)	2.69, br d (12.2)	2.69, dd (12.8, 3.0)
4b	2.83, br d (8.0)	2.85, m	2.65, q (12.0)	2.42, br d (9.6)	2.46, dd (12.8, 3.0)
6	5.75, d (5.4)	5.77, d (5.4)	5.53, d (4.8)	5.25, d (5.4)	5.27, d (4.8)
7a	4.05, br s	3.30, m	1.86, o	1.75, o	1.87, o
7b			1.53, o	1.75, o	1.50, o
8	1.72, o	1.69, o	1.53, o	1.47, o	1.50, o
9	1.64, o	1.55, o	1.37, td (11.0, 4.0)	0.87, o	0.92, o
11a	1.61, o	1.55, o	2.87, br d (4.4)	1.38, o	1.57, o
11b	1.61, o	1.55, o	1.75, o	1.38, o	1.46, o
12a	2.24, td (12.8, 4.6)	2.16, td (13.4, 4.6)	1.82, o	1.72, o	1.50, o
12b	1.55, o	1.49, m	1.28, o	1.12, o	1.50, o
14	3.04, td (12.8, 5.8)	2.83, m	2.02, m	1.06, o	2.07, o
15a	2.72, q (12.8)	2.35, q (12.8)	1.53, o	1.98, o	2.16, o
15b	1.56, o	1.58, o	1.53, o	1.47, o	1.48, o
16	4.55, t (7.2)	4.53, t (7.2)	4.60, t (7.2)	4.61, o	4.49, t (6.6)
17			1.89, m	1.91, m	
18	1.02, s	0.97, s	1.22, s	1.13, s	0.95, s
19	1.09, s	1.04, s	1.27, s	0.83, s	0.91, s
20	2.32, q (7.2)	2.29, q (7.0)	3.26, t (7.2)	3.24, t (6.8)	2.39, q (7.2)
21	1.25, d (7.2)	1.23, d (7.0)	1.19, d (6.6)	1.24, d (7.0)	1.28, d (7.2)
23a	1.70, o	1.72, o	4.06, m	4.06, m	2.42, m
23b	1.70, o	1.72, o	4.06, m	4.06, m	2.11, o
24a	1.72, o	1.55, o	2.42, o	2.41, o	4.55, dd (11.8, 2.4)
24b			1.91, m	1.91, m	
25	1.56, o	1.55, o	1.78, o	1.81, o	2.25, m
26a	3.47, o	3.54, o	3.48, o	3.49, o	4.18, dd (11.2, 4.8)
26b	3.47, o	3.54, o	3.48, o	3.49, o	4.06, o
27a	0.64, d (6.0)	0.67, d (5.0)	0.57, d (5.0)	0.57, d (9.6)	4.38, o
27b					4.03, o
7-O-Me		3.23, s			
3-O-Glc					
1'	4.97, d (7.2)	5.01, d (7.2)		5.04, d (7.6)	5.00, d (5.2)
2'	4.27, o	4.28, o		4.09, o	4.05, o
3'	4.28, o	4.29, o		4.32, o	4.28, o
4'	4.16, t (9.6)	4.20, t (9.6)		4.29, o	4.27, o
5'	3.89, m	3.85, m		4.01, o	3.97, m
6'a	4.52, t (6.8)	4.46, dd (12.0, 2.0)		4.56, o	4.54, dd (11.8, 2.4)
6'b	4.37, o	4.36, o		4.41, o	4.37, o
2'-O-Rha			23-O-Glc	23-O-Glc	
1''	6.38, br s	6.41, br s	5.00, d (7.6)	5.00, d (7.6)	
2''	4.82, br s	4.83, br s	4.02, m	4.04, o	
3''	4.62, m	4.66, dd (9.2, 3.2)	4.24, o	4.28, o	
4''	4.36, t (9.2)	4.37, t (9.4)	4.25, o	4.28, o	
5''	4.99, o	5.00, o	4.00, m	4.01, o	
6''a	1.70, d (6.0)	1.77, d (6.0)	4.53, br d (10.4)	4.56, o	
6''b			4.40, m	4.41, o	

^a s, singlet; d, doublet; t, triplet; q, quartet; br, broad; m, multiplet; o, overlapped.

^b Recorded at 600 MHz.

^c Recorded at 400 MHz.

to silica get CC (CHCl₃:MeOH:H₂O, 10:1:0 → 7:3:0.5, v/v) and followed by semi-preparative HPLC to afford **3** (13.5 mg), **9** (13.4 mg), **10** (1.2 mg), **19** (44.0 mg), **20** (81.3 mg), and **21** (20.0 mg), respectively. Fr. 3.2 (19.5 g) and Fr. 3.4 (10.4 g) were crystallized to afford **14** (12.8 mg) and **16** (20.0 mg), respectively. The mother liquor of Fr. 3.2 was then purified by HPLC (CH₃CN:H₂O, 50:50 → 60:40, v/v) to obtain **1** (12.6 mg), **4** (13.6 mg), **6** (4.2 mg), and **7** (3.3 mg). Similarly, the mother liquor of Fr. 3.4 was further purified by semi-preparative HPLC (CH₃CN:H₂O, 50:50 → 55:45, v/v) to yield **2** (6.5 mg), **5** (3.4 mg), and **8** (24.7 mg).

4.3.1. Trillikamtoside A (**1**)

White amorphous powder; α_D¹⁸ –107 (c 0.10, MeOH); IR (KBr) ν_{max} 3423, 2952, 1636, 1053, 978, 918, 898, 870 cm⁻¹ (intensity: 898 cm⁻¹ > 918 cm⁻¹); for ¹H (pyridine-*d*₅, 600 MHz) and ¹³C NMR

(pyridine-*d*₅, 150 MHz) spectroscopic data, see Tables 1 and 3; EIMS *m/z* 754 [M]⁺; HREIMS *m/z* 754.4162 [M]⁺ (calcd. for C₃₉H₆₂O₁₄, 754.4140).

4.3.2. Trillikamtoside B (**2**)

White amorphous powder; α_D¹⁸ –89 (c 0.16, MeOH); IR (KBr) ν_{max} 3425, 2932, 1634, 1054, 978, 917, 898, 872 cm⁻¹ (intensity: 898 cm⁻¹ > 917 cm⁻¹); for ¹H (pyridine-*d*₅, 600 MHz) and ¹³C NMR (pyridine-*d*₅, 150 MHz) spectroscopic data, see Tables 1 and 3; positive ESIMS *m/z* 923 [M + Na]⁺; positive HRESIMS *m/z* 923.4625 [M + Na]⁺ (calcd. for C₄₅H₇₂O₁₈Na, 923.4616).

4.3.3. Trillikamtoside C (**3**)

White amorphous powder; α_D¹⁸ –86 (c 0.18, MeOH); UV (MeOH) λ_{max} (log ε) 240 (3.7) nm; IR (KBr) ν_{max} 3441, 2951, 1680, 1632, 1054,

Table 3
¹³C NMR spectroscopic data of **1–10** in C₅D₅N.

Position	1 ^a	2 ^a	3 ^b	4 ^a	5 ^a	6 ^a	7 ^a	8 ^b	9 ^b	10 ^a
1	37.8	37.1	34.9	36.8	36.1	37.1	36.9	78.1	37.4	37.4
2	27.8	27.2	26.3	30.3	29.7	29.9	29.9	43.6	30.3	30.1
3	75.2	74.6	74.5	78.2	77.8	77.4	77.5	68.1	78.1	78.0
4	125.8	125.0	130.7	31.2	30.6	38.8	39.0	44.0	39.3	39.2
5	148.7	148.2	147.2	170.3	169.5	143.6	146.0	140.2	140.9	140.7
6	74.1	73.4	203.0	189.8	189.3	125.9	121.2	124.5	121.8	121.6
7	40.8	40.1	46.6	140.4	139.8	64.5	73.6	32.3	32.3	31.9
8	31.6	31.0	34.8	46.8	46.2	38.5	37.7	32.8	31.5	32.2
9	55.3	54.7	51.1	60.6	60.0	42.3	42.9	51.3	50.2	50.5
10	37.9	37.1	38.5	47.0	46.3	37.8	37.9	43.6	37.1	36.9
11	21.4	20.8	20.5	20.8	20.2	20.6	20.6	24.2	21.1	20.8
12	32.5	32.1	31.8	33.0	32.4	31.9	32.0	40.8	40.2	32.2
13	45.5	45.3	45.5	48.4	47.8	44.8	44.8	41.0	41.0	45.1
14	53.1	52.4	52.9	50.9	50.3	46.1	45.5	57.3	56.6	52.3
15	32.2	31.5	31.3	34.9	34.3	32.0	31.8	32.3	32.1	31.6
16	90.5	89.8	90.0	90.4	89.7	90.2	90.0	81.4	81.4	90.2
17	90.4	89.9	90.0	89.5	89.0	90.2	90.1	62.4	62.2	90.0
18	17.8	17.2	17.3	17.8	17.4	17.0	16.7	17.4	17.1	17.0
19	22.0	21.3	19.7	16.0	15.3	18.2	18.2	14.8	19.3	19.3
20	45.3	44.7	44.8	45.1	44.5	44.8	44.8	35.8	35.7	44.9
21	10.3	9.7	9.8	10.5	9.8	9.8	9.7	14.9	14.8	9.7
22	110.3	109.6	109.9	110.1	109.5	109.7	109.7	110.8	110.7	112.0
23	32.5	31.9	32.1	32.6	32.0	31.9	31.8	76.4	76.6	42.0
24	29.3	28.6	28.8	29.3	28.7	28.7	28.7	37.3	37.2	66.3
25	30.9	30.3	30.5	31.0	30.3	30.3	30.3	31.5	31.6	47.6
26	67.1	66.5	66.7	67.1	66.5	66.5	66.5	65.7	65.7	62.2
27	17.9	17.2	17.2	17.8	17.2	17.2	17.2	16.8	16.7	61.4
7-Ome							56.2			
3-O-Glc										
1'	101.5	100.4	101.2	101.3	100.7	100.2	100.4		102.6	102.5
2'	78.6	77.8	78.6	77.7	77.0	77.5	77.7		75.4	75.3
3'	80.2	77.9	79.5	80.1	77.8	79.5	79.5		78.7	78.5
4'	72.1	78.2	71.8	72.2	78.3	71.7	71.5		71.7	71.6
5'	79.0	77.0	78.6	79.0	76.9	78.3	78.1		78.6	78.4
6'	63.1	61.1	62.5	63.1	61.2	62.5	62.3		62.8	62.7
2'-O-Rha								23-O-Glc	23-O-Glc	
1''	102.7	102.1	102.5	102.3	101.6	101.9	101.9	106.3	106.3	
2''	73.2	72.4	72.7	73.0	72.4	72.7	72.7	75.4	75.4	
3''	73.1	72.5	73.0	73.4	72.7	72.5	72.5	78.9	78.7	
4''	75.0	74.3	74.5	74.6	74.0	74.0	74.0	71.6	71.7	
5''	69.6	69.1	69.9	69.9	69.3	69.4	69.4	78.5	78.6	
6''	19.0	18.3	18.6	18.0	18.5	18.6	18.6	62.7	62.8	
4'-O-Rha										
1'''		102.8			102.8					
2'''		72.5			72.5					
3'''		72.6			72.6					
4'''		73.8			73.8					
5'''		70.1			70.3					
6'''		18.4			18.4					

^a Recorded at 150 MHz.^b Recorded at 100 MHz.**Table 4**
Hemostatic and antimicrobial effects of **12–14** and **16–18**.^a

Compounds	Induced-platelet aggregation effect (EC ₅₀ , μM)	Anti- <i>Candida albicans</i> activity (MIC, μM)
12	492.7 ± 33.3	21.1
13	–	10.6
14	203.3 ± 29.9	8.8
16	109.8 ± 45.4	–
17	–	21.6
18	–	11.0
Adenosine diphosphate ^b	53.3 ± 6.5	–
Fluconazole ^b	–	52.3

^a Other compounds were inactive in antimicrobial assay (MIC > 100 μM).^b Positive controls.

978, 916, 900, 865 cm⁻¹ (intensity: 900 cm⁻¹ > 916 cm⁻¹); for ¹H (pyridine-*d*₅, 400 MHz) and ¹³C NMR (pyridine-*d*₅, 100 MHz) spectroscopic data, see [Tables 1 and 3](#); positive ESIMS *m/z* 775

[M + Na]⁺; positive HRESIMS *m/z* 775.3875 [M + Na]⁺ (calcd. for C₃₉H₆₀O₁₄Na, 775.3881).

4.3.4. Trillikamtoside D (4)

White amorphous powder; α_D^{18} -53.2 (c 0.14, MeOH); UV (MeOH) λ_{\max} (log ϵ) 255 (3.7), 202 (3.6) nm; IR (KBr) ν_{\max} 3424, 2930, 1664, 1383, 980, 918, 896, 867 cm^{-1} (intensity: $896 \text{ cm}^{-1} > 918 \text{ cm}^{-1}$); for ^1H (pyridine- d_5 , 600 MHz) and ^{13}C NMR (pyridine- d_5 , 150 MHz) spectroscopic data, see Tables 1 and 3; positive ESIMS m/z 775 $[\text{M} + \text{Na}]^+$; positive HRESIMS m/z 775.3876 $[\text{M} + \text{Na}]^+$ (calcd. for $\text{C}_{39}\text{H}_{60}\text{O}_{14}\text{Na}$, 775.3881).

4.3.5. Trillikamtoside E (5)

White amorphous powder; α_D^{18} -53.7 (c 0.08, MeOH); UV (MeOH) λ_{\max} (log ϵ) 255 (3.5), 202(3.4) nm; IR (KBr) ν_{\max} 3441, 2931, 1638, 1383, 1055, 979, 917, 895, 866 cm^{-1} (intensity: $895 \text{ cm}^{-1} > 918 \text{ cm}^{-1}$); for ^1H (pyridine- d_5 , 600 MHz) and ^{13}C NMR (pyridine- d_5 , 150 MHz) data, see Tables 1 and 3; positive ESIMS m/z 921 $[\text{M} + \text{Na}]^+$; positive HRESIMS m/z 921.4453 $[\text{M} + \text{Na}]^+$ (calcd. for $\text{C}_{45}\text{H}_{70}\text{O}_{18}\text{Na}$, 921.4460).

4.3.6. Trillikamtoside F (6)

White amorphous powder; α_D^{18} -88 (c 0.15, MeOH); IR (KBr) ν_{\max} 3441, 2931, 1631, 1054, 1053, 979, 953, 917, 896, 866 cm^{-1} (intensity: $896 \text{ cm}^{-1} > 917 \text{ cm}^{-1}$); for ^1H (pyridine- d_5 , 600 MHz) and ^{13}C NMR (pyridine- d_5 , 150 MHz) spectroscopic data, see Tables 2 and 3; positive ESIMS m/z 777 $[\text{M} + \text{Na}]^+$; positive HRESIMS m/z 777.4042 $[\text{M} + \text{Na}]^+$ (calcd. for $\text{C}_{39}\text{H}_{62}\text{O}_{14}\text{Na}$, 777.4037).

4.3.7. Trillikamtoside G (7)

White amorphous powder; α_D^{18} -88 (c 0.16, MeOH); IR (KBr) ν_{\max} 3431, 2903, 1631, 1381, 980, 918, 894, 865 cm^{-1} (intensity: $894 \text{ cm}^{-1} > 918 \text{ cm}^{-1}$); for ^1H (pyridine- d_5 , 600 MHz) and ^{13}C NMR (pyridine- d_5 , 150 MHz) spectroscopic data, see Tables 2 and 3; positive ESIMS m/z 791 $[\text{M} + \text{Na}]^+$; positive HRESIMS m/z 791.4188 $[\text{M} + \text{Na}]^+$ (calcd. for $\text{C}_{40}\text{H}_{64}\text{O}_{14}\text{Na}$, 791.4194).

4.3.8. Trillikamtoside H (8)

White amorphous powder; α_D^{18} -45.7 (c 0.10, MeOH); IR (KBr) ν_{\max} 3425, 2903, 1632, 1072, 963, 920, 900, 870 cm^{-1} ; for ^1H (pyridine- d_5 , 400 MHz) and ^{13}C NMR (pyridine- d_5 , 100 MHz) spectroscopic data, see Tables 2 and 3; positive ESIMS m/z 631 $[\text{M} + \text{Na}]^+$; positive HRESIMS m/z 631.3461 $[\text{M} + \text{Na}]^+$ (calcd. for $\text{C}_{33}\text{H}_{52}\text{O}_{10}\text{Na}$, 631.3458).

4.3.9. Trillikamtoside I (9)

White amorphous powder; α_D^{18} -38 (c 0.08, MeOH); IR (KBr) ν_{\max} 3425, 2953, 1632, 1382, 963, 924, 902, 873 cm^{-1} ; for ^1H (pyridine- d_5 , 400 MHz) and ^{13}C NMR (pyridine- d_5 , 100 MHz) spectroscopic data, see Tables 2 and 3; positive ESIMS m/z 777 $[\text{M} + \text{Na}]^+$; positive HRESIMS m/z 777.4045 $[\text{M} + \text{Na}]^+$ (calcd. for $\text{C}_{39}\text{H}_{62}\text{O}_{14}\text{Na}$, 777.4037).

4.3.10. Trillikamtoside J (10)

White amorphous powder; α_D^{18} -70.3 (c 0.18, MeOH); IR (KBr) ν_{\max} 3427, 2930, 1632, 1380, 978, 903 cm^{-1} ; for ^1H (pyridine- d_5 , 600 MHz) and ^{13}C NMR (pyridine- d_5 , 150 MHz) spectroscopic data, see Tables 2 and 3; positive ESIMS m/z 647 $[\text{M} + \text{Na}]^+$; positive HRESIMS m/z 647.3397 $[\text{M} + \text{Na}]^+$ (calcd. for $\text{C}_{33}\text{H}_{52}\text{O}_{11}\text{Na}$, 647.3407).

4.4. Determination of absolute configuration of sugars by HPLC

The absolute configurations of the sugar moieties were determined by the method described in the literature (Born, 1962; Born and Cross, 1963). Standard monosaccharides, L-rhamnose (5 mg) and D-glucose (5 mg), were incubated with L-cysteine methyl ester hydrochloride (5 mg) (Aldrich, Japan) in pyridine (5 mL)

respectively. After heating at 60 °C for 1 h, *o*-tolyl isothiocyanate (10 μL) (Tokyo Chemical Industry Co., Ltd., Japan) was next added to each and the solutions were kept at 60 °C for 1 h. The products of D-glucose and L-rhamnose were separated by silica gel CC (200–300 mesh) eluted with CHCl_3 and $\text{CHCl}_3:\text{MeOH}$ (100:1, v/v) to remove the low polar by-products independently, while $\text{CHCl}_3:\text{MeOH}$ (100:1, v/v) and $\text{CHCl}_3:\text{MeOH}$ (30:1, v/v) were employed to afford the target products methyl 2-(polyhydroxyalkyl)-3-(*o*-tolylthiocarbonyl)-thiazolidine-4(*R*)-carboxylates. The products were further confirmed by their peaks at m/z 469 $[\text{M} + \text{Na}]^+$ and 455 $[\text{M} + \text{Na}]^+$ in the ESI-MS. Analytical HPLC was performed on a ZORBAX SB-C₁₈ column (250 \times 4.6 mm i.d., 5 μm , Agilent, U.S.A) at 35 °C with gradient elution of $\text{CH}_3\text{CN}:\text{H}_2\text{O}$ (20:80 \rightarrow 50:50, v/v) for 30 min at a flow rate of 1 mL/min. Peaks were detected by UV detection at 254 nm, with peaks of standard monosaccharide derivatives recorded at t_R 13.83 (D-Glc), t_R 17.74 (L-Rha).

Compounds 1–10 (1 mg, each) were individually treated with 6 M CF_3COOH (1,4-dioxane/ H_2O 1:1, 1 mL) under conditions of refluxing on a water bath for 2 h at 90 °C. After cooling, each reaction mixture was extracted with CHCl_3 (3 \times 5 mL). Next, each aqueous layer was evaporated to dryness using rotary evaporation. Each dried residue was dissolved in pyridine (1 mL) mixed with L-cysteine methyl ester hydrochloride (1 mg) (Aldrich, Japan) and heated at 60 °C for 1 h. Then, *o*-tolyl isothiocyanate (5 μL) (Tokyo Chemical Industry Co., Ltd., Japan) was added to each mixture, this being heated at 60 °C for 1 h. Each reaction mixture was directly analyzed by reversed phase HPLC following the above procedure. Under these conditions, the absolute configurations of the sugars for ten new saponins were identified as D-glucose ($t_R = 13.90$ min) and L-rhamnose ($t_R = 17.66$ min), respectively.

4.5. Platelet aggregation assays

Turbidometric measurements of platelet aggregation of the samples were performed in a Chrono-log Model 700 Aggregometer (Chrono-log Corporation, Havertown, PA, USA) according to Born's method (Born, 1962; Born and Cross, 1963). Platelet aggregation studies were completed within 3 h of preparation of PRP. Immediately after preparation of PRP, 250 μL was incubated in each of the test tubes at 37 °C for 5 min and then 2.5 μL of compounds (300 $\mu\text{g}/\text{mL}$) were individually added. The changes in absorbance as a result of platelet aggregation were recorded. The extent of aggregation was estimated by the percentage of maximum increase in light transmittance, with the buffer representing 100% transmittance. ADP (Adenosine diphosphate) was used as a positive control with a $53.3 \pm 6.5\%$ maximal platelet aggregation rate at a concentration of 10 μM . 1% DMSO was used as a blank control with a 3.0% maximal platelet aggregation. Data counting and analysis was done on SPSS 16.0, with experimental results expressed as mean \pm standard error.

4.6. Antimicrobial assays

Four bacterial strains: *Candida albicans* (ATCCY0109), *Staphylococcus aureus* (ATCC25913), *Escherichia coli* (ATCC25922), and *Pseudomonas aeruginosa* (ATCC27853) (Chinese Food and Drug Inspection Institute) were cultivated in ordinary AGAR medium (*C. albicans* was cultivated in Solid Sabouraud Medium) at 37 °C for 24 h and then transplanted *in vitro*. The final concentration of the suspension was adjusted to 10^6 CFU/mL by direct microscopic counts. The MIC (minimal inhibitory concentration) of the samples against the bacterial and fungal strains was determined according to America Clinical and Laboratory Standards Institute, using the micro liquid dilution method. The MIC is defined as the minimum concentration of the compounds at which the microorganisms do

not demonstrate visible growth. In order to determine MIC values of the test compounds, ten two-fold serial dilutions were performed for each compound. Culture media (100 μL) were placed in a 96-well micro-titer plate in 1–12 holes. Test compounds were dissolved in DMSO (100 μL) and then added to the second hole of each row containing already placed culture media (100 μL). After blending, a 100 μL of the mixture from second hole was moved to third hole, and so on for times until the 11th hole. A 100 μL mixture taken from 11th hole was not put in 12th hole, instead, it was discarded. Finally, bacteria or fungi suspension of 100 μL was placed in 2–12 holes. In this way, every first hole of the row contained only culture media as sterility check while every 12th hole of the row contained only bacterial/fungal liquid as negative control. The plate was incubated under anaerobic condition at 37 °C for 24 h. After incubation, the wells were examined for growth of microorganisms and the MIC values were determined. Each experiment was repeated three times. MIC > 100 μM were considered to be inactive.

Fluconazole and vancomycin were used as positive controls, with MIC values of 52.3 and 0.7 μM against *C. albicans* and *Staphylococcus aureus*, respectively, while amikacin was used as the positive control with MIC values of 3.4 and 1.7 μM against *E. coli* and *P. aeruginosa*, respectively.

Acknowledgments

This work was supported financially by the National Natural Science Funding of China (Nos. 31600283 and 31570363) and the Natural Science Foundation of Yunnan Province (No. 2015FA031).

Appendix A. Supplementary data

Supplementary data related to this article can be found at <http://dx.doi.org/10.1016/j.phytochem.2016.09.006>.

References

- Asano, T., Murayama, T., Hirai, Y., Shoji, J., 1993. Comparative studies on the constituents of ophiopogon tuber and its congeners. VIII. Studies on the glycosides of the subterranean part of *Ophiopogon japonicus* Ker-Gawler cv. Nanus. (2). Chem. Pharm. Bull. 41, 566–570.
- Born, G.V.R., 1962. Aggregation of blood platelets by adenosine diphosphate and its reversal. Nature 194, 927–929.
- Born, G.V.R., Cross, M.J., 1963. The aggregation of blood platelets. J. Physiol. 168, 178–195.
- Chen, C.X., Zhang, Y.T., Zhou, J., 1981. Studies on the saponin components of plants in Yunnan steroid glycosides of *Paris polyphylla* SM. var. *yunnanensis* (Fr.) H–M. (2). Acta Bot. Yunnan. 5, 91–97.
- Hayes, P.Y., Lehmann, R., Penman, K., Kitching, W., De Voss, J.J., 2009. Steroidal saponins from the roots of *Trillium erectum* (Beth root). Phytochemistry 70, 105–113.
- Jiangsu New Medical College, 1975. Dictionary of Chinese Traditional Medicine (Zhong Yao Da Ci Dian). Shanghai Science and Technology Press, Shanghai, p. 83.
- Kasai, R., Okaiharu, J., Asakawa, J., Mizutani, K., Tanaka, O., 1979. ^{13}C NMR study of α - and β -anomeric pairs of D-mannopyranosides and L-rhamnopyranosides. Tetrahedron 35, 1427–1432.
- Lu, Y., Chen, C.X., Ni, W., Huan, Y., Liu, H.Y., 2010. Spirostanol tetraglycosides from *Ypsilandra thibetica*. Steroids 95, 982–987.
- Mahato, S.B., Sahu, N.P., Ganguly, A.N., 1981. Steroidal saponins from *Dioscorea floribunda*: structures of floribundasaponins A and B. Phytochemistry 20, 1943–1946.
- Mimaki, Y., Kuroda, M., Kameyama, A., Yokosuka, A., Sashida, Y., 1998. Aculeoside B, a new bisdesmosidic spirostanol saponin from the underground parts of *Ruscus aculeatus*. J. Nat. Prod. 61, 1279–1282.
- Mimaki, Y., Kuroda, M., Obata, Y., Sashida, Y., Kitahara, M., Yasuda, A., Naoi, N., Xu, Z.W., Kawano, S., Lao, A.N., 2000. Steroidal saponins from the rhizomes of *Paris polyphylla* var. *chinensis* and their cytotoxic activity on HL-60 cells. Nat. Prod. Lett. 14, 357–364.
- Nohara, T., Miyahara, K., Kawasaki, T., 1975. Steroid saponins and sapogenins of underground parts of *Trillium kamschaticum* Pall. II. Pennogenin- and kryptogenin 3-O-glycosides and related compounds. Chem. Pharm. Bull. 23, 872–885.
- Ohara, M., Kawano, S., 2005. Life-history monographs of Japanese plants. 2: *Trillium kamschaticense* Ker-Gawl. (Trilliaceae). Plant. Spec. Biol. 20, 75–82.
- Ono, M., Yanai, Y., Ikeda, T., Okawa, M., Nohara, T., 2003. Steroids from the underground parts of *Trillium kamschaticum*. Chem. Pharm. Bull. 51, 1328–1331.
- Ono, M., Takamura, C., Sugita, F., Masuoka, C., Yoshimitsu, H., Ikeda, T., Nohara, T., 2007. Two new steroid glycosides and a new sesquiterpenoid glycoside from the underground parts of *Trillium kamschaticum*. Chem. Pharm. Bull. 55, 551–556.
- Qin, X.J., Sun, D.J., Ni, W., Chen, C.X., Hua, Y., He, L., Liu, H.Y., 2012. Steroidal saponins with antimicrobial activity from stems and leaves of *Paris polyphylla* var. *yunnanensis*. Steroids 77, 1242–1248.
- Qin, X.J., Chen, C.X., Ni, W., Yan, H., Liu, H.Y., 2013. C₂₂-steroidal glycosides from stems and leaves of *Paris polyphylla* var. *yunnanensis*. Fitoterapia 84, 248–251.
- Sun, C.L., Ni, W., Yan, H., Liu, Z.H., Yang, L., Si, Y.A., Hua, Y., Chen, C.X., He, L., Zhao, J.H., Liu, H.Y., 2014. Steroidal saponins with induced platelet aggregation activity from the aerial parts of *Paris verticillata*. Steroids 92, 90–95.
- Wang, F.C., Tang, J., Chen, X.Q., Zhang, Z.Y., Dai, L.K., Liang, S.Y., Tang, Y.C., Liu, L., Lang, K.Y., 1978. Flora of China, vol. 15(2). Science Press, Beijing, pp. 97–98.
- Yokosuka, A., Mimaki, Y., 2008. Steroidal glycosides from the underground parts of *Trillium erectum* and their cytotoxic activity. Phytochemistry 69, 2724–2730.
- Yu, L.L., Zou, K., Wang, X.Z., Zhu, L.L., Zhou, Y., Yang, J., 2008. Study on the anti-inflammatory, analgesic and thrombosis effects of extract of *Trillium tschonoskii* Maxim. Lishizhen Med. Mater. Med. Res. 19, 1178–1180.
- Zhang, M., Li, Z.Y., Liao, C.L., Zhou, F.Q., Li, Y.W., Cui, J., 2011. Textual research and pharmacognosic identification of ethnic-medicine *Rhizoma et Radix Trillii*. Lishizhen Med. Mater. Med. Res. 10, 2504–1180.
- Zhang, X.D., Chen, C.X., Yang, J.Y., Ni, W., Liu, H.Y., 2012. New minor spirostane glycosides from *Ypsilandra thibetica*. Helv. Chim. Acta 95, 1087–1093.